IOSR Journal of Engineering (IOSRJEN) **www.iosrjen.org**
ISSN (e): 2250-3021, ISSN (p): 2278-8719
Vol. 11, Issue 8, August 2021, ||Series -I|| PP 34-38

Growth and characterization of tungsten titanium nanoparticles (WTi) produced by DC magnetron sputtering

A. AL-Rjoub[1], L. Rebouta[1]
[1](Physics Center of Minho and Porto Universities - CF-UM-UP, University of Minho, Campus de Azurém, 4800-058 Guimarães, Portugal)
Corresponding Author: A. AL-Rjoub
Received 20 July 2021; Accepted 5 August 2021

Abstract : In this study, a description procedure of WTi nanoparticles produced by DC magnetron sputtering in a plasma-gas-condensation cluster source is presented. After optimizing the parameters of the nanoparticles' formation, they were characterized by Scanning Electron Microscopy (SEM), Energy Dispersive Spectrometer (EDS), X-ray Diffraction (XRD) and Transmission Electron Microscopy (TEM). The deposition Rate of the nanoparticles is 240 nm/min, which is relatively high, and their diameters ranged between 20 – 60 nm. All analyzed samples contain oxygen as confirmed by EDS analysis. XRD and TEM analyses emphasize the crystalline structure of the nanoparticles with a dominant α- W phase structure.
Keywords: - About WTi nanoparticles, TEM analysis, Sputtering.

I. INTRODUCTION

Recently, hybrid metallic nanoparticles (NPs) have been widely used in enormous applications. Their size dependent on physical and chemical properties made them excellent candidates for optical, electrical, magnetic, biomedicine and chemical applications [1-3]. For examples, they can be used as catalysis reaction due to their high surface to volume ratio. Also, they were used in photovoltaic cells, sensors, memories, lithium batteries, single electron devices as quantum dots and spintronic applications [4-9]. Moreover, ceramic solar thermal absorber stacks-based structure on metal oxides and metal nanoparticles such as tungsten or titanium nanoparticles show an excellent thermal stability and high oxidation resistance [10].

Nanoparticles can be produced using different methods and process, such as gas condensation, chemical vapor synthesis, solvothermal decomposition, mechanical milling, chemical precipitation, Sol-Gel technique, electrodeposition, molecular beam epitaxy, ionised cluster beam, liquid metal ion source, consolidation, gas aggregation of monomers chemical precipitation in presence of capping agents and magnetron sputtering [1,9,11-13]. In general, the growth rate of nanoparticles varies widely according to used material [14], but the chemical processes have higher production rate and generally less purity comparing with physical methods such as sputtering. However, the selection method of nanoparticles depends on the wanted application.

In this paper, a magnetron sputtering based nanocluster source by gas condensation with Ar as sputtered gas was used to produce tungsten titanium nanoparticles (WTi), which can be used in ceramic solar radiation absorbers for high temperature applications. These absorbers are usually a multilayer stack, whit two absorption layers, consisting of hybrid metallic nanoparticles (PNs) embedded in a ceramic matrix, with a high and low metal volume fraction (e.g W, WTi or other metals). The formation conditions and controlling parameters of WTi nanoparticles are studied in detail, such as the nozzle diameter between main and sputtering chambers, the applied current to the target, the distance between target surface and nozzle (growth region) and working pressure. Morphology, microstructure, crystalline structure, and chemical composition of resulting nanoparticles were studied by Scanning Electron Microscopy (SEM), Energy Dispersive X-Ray Spectroscopy (EDS), X-ray Diffraction (XRD) and Transmission Electron Microscopy (TEM).

II. MATERIALS AND METHODS

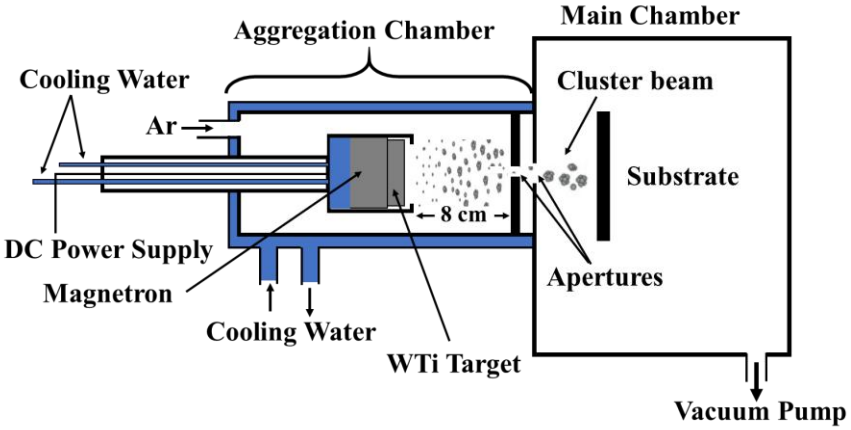

Figure 1: *Schematic* figure of the nanoparticles production system.

WTi nanoparticles were produced by DC magnetron sputtering in a gas aggregation chamber and were deposited on p-doped Boron Si (100) (used for SEM, EDS and XRD), and on CF 400-Cu grids carbon film, 400 mesh copper (used for TEM). Fig. 1 presents the schematic figure of the deposition system where the depositions were performed. The system is divided into two main parts: i) the main chamber that contains the substrates holder. This chamber is equipped with a vacuum system that can reach a base pressure of 1×10-4 Pa, and ii) the gas aggregation chamber that contains a magnetron supported with water cooling system as shown in the figure. The two chambers are connected by a nozzle with two apertures with diameters 2.5 mm and 4 mm, respectively, to guarantee the flow direction of the cluster beams toward the main chamber due to pressure differences. The depositions were performed by applying a current density of 2.7 mA/cm2 on a W: Ti (90:10) at.% composite target of 69 mm in diameter. Ar was used as sputtering gas with flow of 14 sccm resulting a working pressure of 0.43 Pa and 1.1 Pa in the main and the aggregation chambers, respectively. The deposition times on grids and on Si substrates were 5 s and 10 min, respectively. Before the deposition, silicon substrates were ultrasound cleaned in acetone and in alcohol for 15 min.

Scanning electron microscopy analysis was performed in a NanoSEM-FEI Nova 200 (FEG/SEM) equipment, to determine the coatings' thickness and morphology of the thick layers deposited on Si substrates. EDS analyses were performed with the electron beam of the SEM and a EDAX - Pegasus X4M system. The measurements were randomly performed on the sample surface with an acceleration voltage of 25 keV. The crystalline structure of the coating was studied using X-ray diffraction employing a Bruker AXS Discover D8, operating with CuKα radiation. X-Ray diffraction measurements were performed using a 3º incidence angle.

TEM analysis were performed using high resolution Energy Filtered 200 kV Transmission Electron Microscope HR-(EF)TEM JEOL 2200FS of the RNME-UA, supported on the long standing Schottky emission gun SEG and the high precision slow scan SCCD camera, offers state-of-the art analytical electron microscopy at 0.19 nm point/ 0.10 nm lattice resolution of TEM image and in-column Omega filter technology that allows users to obtain energy filtered images (EF-) with inelastic scattering, plasmon or chemical bond contrast, and electron energy loss spectra (EELS) for enhanced elemental and chemical analysis and mapping, equipped with energy dispersive X-Ray microanalysis /EDS.

III. RESULTS AND DISCUSSION

3.1 Chemical composition and structure of thick layer of WTi nanoparticles

The cross-section of thick films of WTi nanoparticles deposited on Si substrates is shown in Fig. 2a and b. The morphological nanoparticles features and the sizes is almost inhomogeneous and it is similar to pure W nano-particles studied by Acsente et al. [9]. The deposition rate of WTi nanoparticles is 240 nm/min, which is slightly high. The chemical composition of this film evaluated by EDS (Table 1) reveals that the O at.% in the film is high due to the high base pressure in the aggregation chamber. As a result, the residual oxygen can easily be incorporated in the grown WTi nanoparticles. The purity can be improved by having a better base pressure in the aggregation chamber.

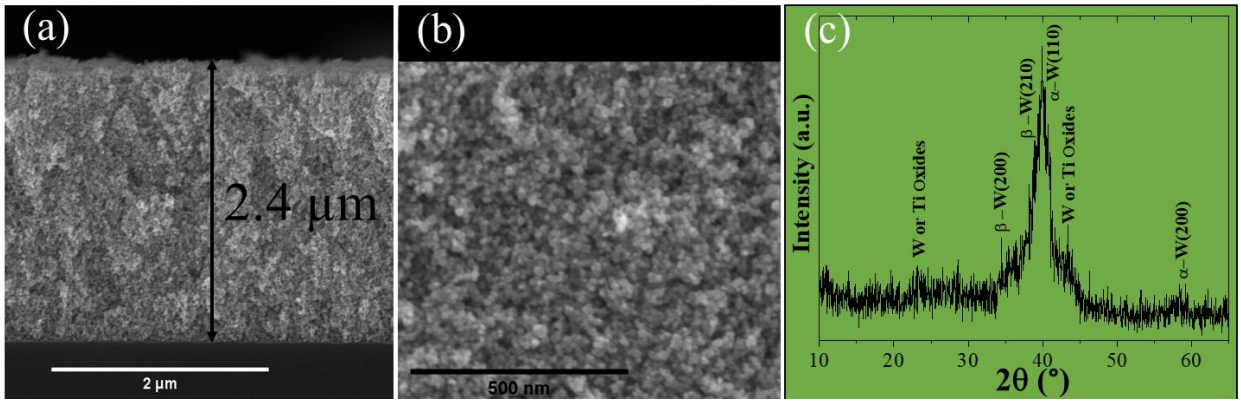

Figure 2: a) Cross-section SEM image of thick film of WTi nanoparticles with b) a magnified zone. c) X-ray diffraction pattern of the thick layer of WTi nanoparticles deposited on Si substrate for 10 min.

Table 1: Chemical composition of WTi nanoparticles thick layer deposited on Si evaluated by EDS analysis.

W at.%	Ti at.%	O at.%
42	28	30

X-ray diffraction (XRD) pattern is shown in Fig. 2c. The coating exhibits the combination of dominant crystalline structure of α- W with the highest peak intensity located θ ≈ 40° and β-W phase structure. The peaks are not very intense due to the partial formation of W and Ti oxides, which are also detected in the X-ray diffraction pattern.

3.2 TEM analysis

A low magnification TEM image of the WTi nanoparticles is shown in Fig. 3a and b. The obtained nano WTi particles have different sizes and shapes with particles diameters ranged between 20- 60 nm (Fig. 3b). The shapes are irregular and/or even not symmetric, showing that these clusters are the result of the aggregation of several smaller nanoparticles. Further structural analysis of those nanoparticles was achieved using high-resolution transmission electron microscopy (HRTEM) images as shown in Fig. 3c. The analysis informs the features of the lattice fringes with dominant and clear interplanar space corresponding to (110) α- W phase, confirming the crystalline nature of the W nanoparticles, which agrees well with the XRD analysis of the thick layers deposited on Si substrate.

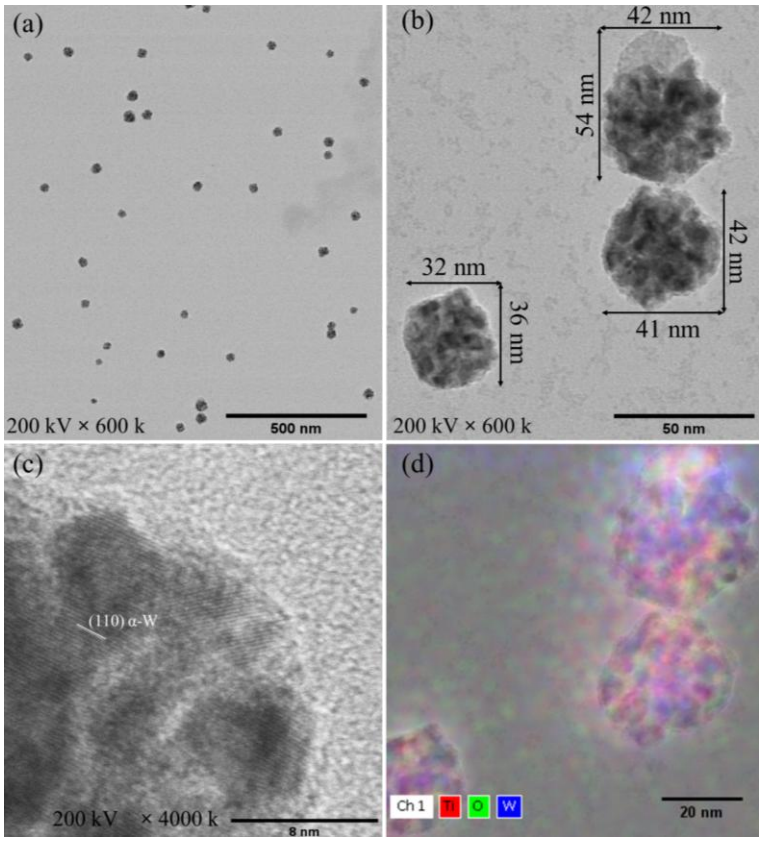

Figure 3: a) and b) Low magnification of the TEM image of WTi nanoparticles, c) High-resolution transmission electron microscopy (HRTEM) and d) TEM energy dispersive microanalysis of X-Rays/EDS of WTi nanoparticles deposited on CF 400-Cu grids for 5s.

Additionally, the energy dispersive spectrometer (EDS) mapping shown in Fig. 3d indicates that the produced nanoparticles mainly consist of W, Ti and O with good agreement of EDS analysis of the thick layer as presented in Table 1. A very thin oxide layer forms at the surface of the particles, which explains the more transparent parts of the boundaries of the nanoparticle [9].

IV. CONCLUSION

Several parameters of WTi nanoparticles production by DC sputtering in a nanocluster source are studied to determine the best conditions for the nano-particles formation and for aggregation, controlling their shapes, sizes and structure. The resulting nanoparticles have high deposition rate 240 nm/min, and their diameters ranged between a 20- 60 nm. The produced nanoparticles contain high concentration of oxygen as confirmed by EDS analysis. XRD and TEM analyses confirm the crystalline structure of the nanoparticles with the dominant α-W phase structure.

ACKNOWLEDGEMENTS

The authors acknowledge the support of FCT in the framework of the Strategic Funding UID/FIS/04650/2013 and the financial support of FCT, POCI and PORL operational programs through the project POCI-01-0145-FEDER-016907 (PTDC/CTM-ENE/2882/2014), co-financed by European community fund FEDER.

REFERENCES

[1] P.K. Sahoo, S.S. Kalyan Kamal, M. Premkumar, T. Jagadeesh Kumar, B. Sreedhar, A.K. Singh, S.K. Srivastava, K. Chandra Sekhar, Synthesis of tungsten nanoparticles by solvothermal decomposition of tungsten hexacarbonyl, *Int. J. Refract. Met. Hard Mater. 27*, 2009, 784–791.

[2] M.A. Syed, U. Manzoor, I. Shah, H.A. Bukhari, Antibacterial effects of Tungsten nanoparticles on the Escherichia coli strains isolated from catheterized urinary tract infection (UTI) cases and Staphylococcus aureus, *New Microbiol. 33*, 2010, 329–335.

[3] O. V Salata, Applications of nanoparticles in biology and medicine, *J. Nanobiotechnology. 2*, 2004, 1–6.

[4] L. Qi, P.H. McMurry, D.J. Norris, S.L. Girshick, Impact dynamics of colloidal quantum dot solids,

Langmuir. *27*,2011, 12677–12683.
[5] M. Nagao, A. Hayashi, M. Tatsumisago, High-capacity Li2S–nanocarbon composite electrode for all-solid-state rechargeable lithium batteries, *J. Mater. Chem. 22*, 2012, 10015.
[6] N. Garg, A. Mohanty, N. Lazarus, L. Schultz, T.R. Rozzi, S. Santhanam, L. Weiss, J.L. Snyder, G.K. Fedder, R. Jin, Robust gold nanoparticles stabilized by trithiol for application in chemiresistive sensors, *Nanotechnology. 21*, 2010, 405501–405507.
[7] P.S.K. Karre, M. Acharya, W.R. Knudsen, P.L. Bergstrom, Single electron transistor-based gas sensing with tungsten nanoparticles at room temperature, *IEEE Sens. J. 8*, 2008, 797–802.
[8] G. Gay, D. Belhachemi, J.P. Colonna, S. Minoret, P. Brianceau, D. Lafond, T. Baron, G. Molas, E. Jalaguier, A. Beaurain, B. Pelissier, V. Vidal, B. De Salvo, Passivated TiN nanocrystals/SiN trapping layer for enhanced erasing in nonvolatile memory, *Appl. Phys. Lett. 97*, 2010, 1–4.
[9] T. Acsente, R.F. Negrea, L.C. Nistor, C. Logofatu, E. Matei, R. Birjega, C. Grisolia, G. Dinescu, Synthesis of flower-like tungsten nanoparticles by magnetron sputtering combined with gas aggregation, *Eur. Phys. J. D*. 69, 2015.
[10] X. Wang, J. Gao, H. Hu, H. Zhang, L. Liang, K. Javaid, High-temperature tolerance in WTi-Al2O3 cermet-based solar selective absorbing coatings with low thermal emissivity, *Nano Energy. 37*, 2017, 232–241.
[11] N. Rajput, Methods of preparation of nanoparticles-A Review, *Int. J. Adv. Eng. Technol. 8*, 2013, 5–19.
[12] H. Lei, Y.J. Tang, J.J. Wei, J. Li, X.B. Li, H.L. Shi, Synthesis of tungsten nanoparticles by sonoelectrochemistry, *Ultrason. Sonochem. 14*, 2007, 81–83.
[13] J. Yu, E.G. Wang, X.D. Bai, Electron field emission from carbon nanoparticles prepared by microwave-plasma chemical-vapor deposition, *Appl. Phys. Lett. 78* (2001, 2226–2228.
[14] D. Samsonov, J. Goree, Particle growth in a sputtering discharge, *J. Vac. Sci. Technol. 17*, 1999, 2835–2840.

A. AL-Rjoub. "Growth and characterization of tungsten titanium nanoparticles (WTi) produced by DC magnetron sputtering." *IOSR Journal of Engineering (IOSRJEN)*, 11(08), 2021, pp. 34-38.